Effect of swaging and mechanical surface treatments on the mechanical properties of the spray-formed ultra high strength copper alloy CuMn20Ni20

I. Altenberger[1], M. Mhaede[2], H.-A. Kuhn[1], Y. Sano[3], L. Wagner[2]

1 Wieland-Werke AG, Central Laboratory,Ulm, Germany
2 Clausthal University of Technology, Institute of Materials Science & Engineering, Germany
3 Toshiba Corporation, Yokohama, Japan

Abstract
The precipitation hardened ordered copper-based alloy CuMn20Ni20 is used as a non-magnetic high strength alloy in offshore- and onshore oil drilling exploration. In spite of already excellent mechanical properties, mechanical enhancement methods such as swaging, deep rolling (ball burnishing), shot peening or laser peening remain attractive for enhancing mechanical properties, especially under fatigue conditions. In the following contribution the effects of swaging, shot peening, deep rolling and laser peening on the high cycle fatigue strength of CuMn20Ni20 were investigated. The present study suggests that these treatments can further increase the fatigue strength and hardness of CuMn20Ni20. The contributing strengthening mechanisms are discussed through applying Electron Channeling Contrast Imaging (ECCI) and electron backscatter diffraction (EBSD) in scanning electron microscopy.

Keywords Cu-alloy, swaging, laser peening, shot peening, deep rolling, EBSD

Introduction

For oil drilling exploration, the non-magnetic spray-formed copper alloy CuMn20Ni20 offers an interesting combination of properties, e.g. high strength, high ductility and good corrosion resistance. CuMn20Ni20 (Wieland designation: LV7) has comparable mechanical properties to high strength steel, titanium alloys or Cu-Be-alloys. It is non-magnetic making it attractive for oil-drilling equipment containing sensors and electronics for orientation purposes. Further applications are profiles in textile industry. Due to the high alloy content LV7 is difficult to produce by conventional casting, therefore it is spray formed into semi-finished products.
CuMn20Ni20 is an age-hardenable alloy, hence appropriate heat treatment can tailor the desired mechanical properties. In a 20% cold-worked and fully aged hardened condition ultimate tensile strengths of almost 1300 MPa are reached. Alternatively, in the more ductile condition elongations to fracture of 18-30% can be achieved, however, at the expense of tensile- as well as yield strength [1,2]. The very high mechanical strengths are achieved by a solution treatment in the α-region, followed by quenching and and relatively long artificial aging treatments. Microscopically, tetragonal and ordered MnNi-precipitates are serving as dislocation obstacles and thus increase the yield- and tensile strength [2]. These precipitates are nanoscopically small rendering them usually invisible in light microscopical micrographs. At grain boundaries discontinuous precipitation occurs during ageing. Compared to Cu-Be-alloys, CuMn20Ni20 can be produced in a wider range of mechanical properties, maintaining substantial ductility at high strength.

Experimental Methods

Backscatter micrographs of the investigated microstructures were taken by using an angle selective backscatter detector in a ZEISS Ultra scanning electron microscope (SEM), equipped with a thermal field emission cathode. For Electron Channeling (ECCI) contrast [3] an angle selective detector was used. Typically, acceleration voltages of 15 - 20 kV and an aperture of 120 microns were used [3,4]. These adjustments were also used for the electron backscatter (EBSD) investigations, where an EBSD-unit by Oxford, was applied. For registration and indexing of the Kikuchi-patterns the commercial software AZTEC was used. Prior to characterization by SEM/EBSD the specimens were carefully ground up to 2400, then polished up to 1 micron and finally vibration-polished using a magnesium oxide suspension in order to minimize near-surface cold-work.

Fatigue tests were performed on hour-glass shaped specimens with 6 mm minimum gage diameter in rotating beam loading (R = -1) in air at a frequency of 50 s^{-1}. A mechanically polished (MP) condition was used as a reference to which the various mechanically surface treated conditions were compared.

Laser peening (LSP) was carried out using a method described in [5,6]. (LSP was performed on the as-machined specimens at Toshiba, Yokohama. The process parameters were: 50 mJ pulse energy, 0.4 mm focal spot diameter and 119 pulses/mm^2 irradiation density. Shot peening was done using a direct pressure blast system of OSK at IWW of TU Clausthal. Spherically conditioned cut wire (SCCW14) having an average diameter of 0.35 mm was used. All peening was performed to full (100 %) coverage at an Almen intensity of 0.20 mmA. Deep rolling was performed at IWW of TU Clausthal by using a conventional lathe and a hydrostatic device from Ecoroll AG, Celle.

A hard metal ball of Ø 6 mm (HG 6) was utilized at a working pressure of 300 bar. Swaging was carried out by using a rotary swaging device. The logarithmic strain by diameter reduction was -2,2.

Experimental Results

Table 1. exhibits the hardness of CuMn20Ni20 in the solution annealed condition (the initial condition was spray formed and hot extruded) as well as in the swaged and swaged plus subsequently aged (7h/450°C) condition. The solution annealed condition is characterized by a low hardness of 95 HV30. This hardness is almost tripled after swaging, and another increase by 200-220 HV30 is reached after optimized artificial aging. The final hardness of around 500 HV30 in the peak-aged condition corresponds to a tensile strength and yield strength of 1525 MPa and 1465 MPa, respectively, at elongations of 1,1%. Fig. 1 shows that an aging temperature of 450°C leads to a maximum hardness increase in the swaged condition. Fig. 2 shows micrographs of the hot extruded plus subsequently aged condition as well as of the swaged plus subsequently aged condition. At this magnification, the grain structure and deformation (slip lines) by swaging is visible, but no precipitates are visible owing to the nano-size of the ordered MnNi precipitates. Further insight into the microstructure can be obtained by ECCI and EBSD (Figs. 3-5, see [7-9] for application of EBSD/ECCI for high strength Cu-Ni-Si alloys). Swaging caused pronounced plasticity within the grains. The mechanisms are slip as well as twinning. Orientation mappings and misorientation measurements by EBSD, identifying $\Sigma 3$-twin boundaries, confirmed that the curved lamellae within the grains are deformations twins (Figs. 4, 5). The nature of the slip was less planar and more wavy than in brass, although some planar slip was also observed (Fig. 3). Due to the generated twin boundaries (in addition to an increase of dislocation density) hardness increases, moreover, the twins appear to be preferential sites for the subsequent formation of nanoscale precipitates during artificial aging (Fig. 3, ECCI-contrast). In summary, after swaging and aging, this highly twinned microstructure containing very small precipitates (diameter < 20 nm) reaches a hardness of 480-505 HV30. After swaging the alloy exhibited an elongation to fracture of 5 %, after peak aging this ductility was reduced to 1.1%. In spite of this hardness increase, the fatigue strength –unlike the tensile strength- did not profit much from aging. The only-aged condition showed a 10^7-fatigue strength of 225 MPa, whereas the swaged plus peak aged condition showed a 10^7-fatigue strength of 270 MPa. This corresponds to 0.2-0.25 σ_{yield}. This disappointing fatigue strength is assumed to be due to the low ductility of fully aged CuMn20Ni20, partially also caused by discontinuous grain boundary precipitates which serve as “internal notches” or local stress raisers and preferred crack initiation sites during fatigue. It is obvious, that a through-thickness hardening by aging/swaging does not lead to a superb fatigue behavior.

Table 1. Hardness of CuMn20Ni20 after solution annealing (1h/850°C) and water quenching, swaging and swaging plus aging (7h/450°C)

solution annealed	95 HV30
solution annealed + swaged	285 HV30
solution annealed + swaged + aged	480 HV30

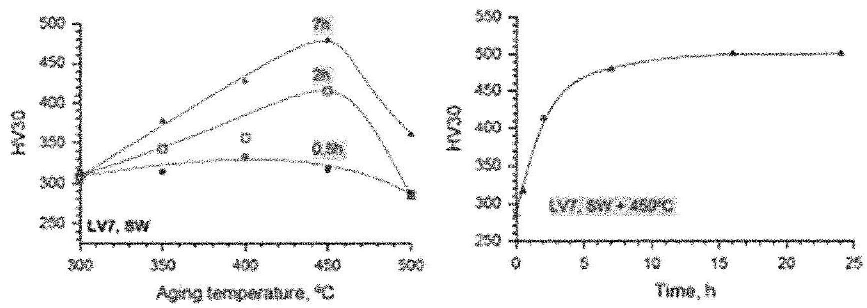

Fig. 1 Aging behaviour of the swaged condition for different aging temperatures

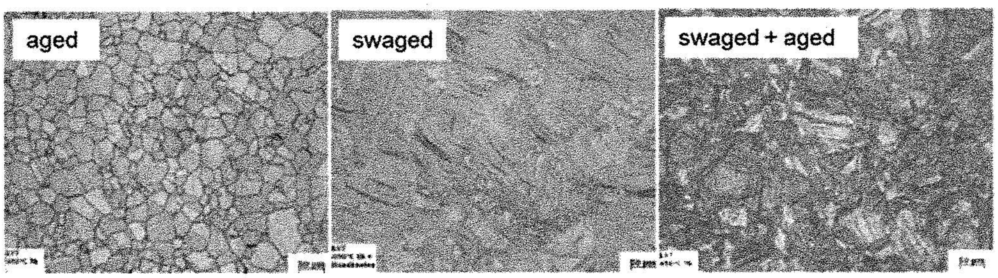

Fig. 2 Microstructure of the aged, swaged and swaged plus aged condition (light-microscopical micrographs)

In light of these results, it would seem reasonable to compensate the brittle behavior of peak-aged CuMn20Ni20 by embedding the potential crack initiation sites and fatigue microcracks into a field of compressive residual stress which can be easily generated by mechanical surface treatments such as shot peening [10], deep rolling [11-13] or by new treatments such as laser peening [14]. Fig. 6 shows the surface hardness increase by laser peening (method by [5]) for the spray formed copper alloys CuMn20Ni20, CuNi7Si2Cr and CuAl13Fe4Mn1Co. In contrast to hardened steels mechanical surface treatments do not lead to near-surface softening, but to work hardening. Fig. 7 shows the effect of laser peening, shot peening and deep rolling on the stress-life behavior of precipitation hardened (hot extruded plus air cooled) CuMn20Ni20. Now, 10^7-fatigue strengths of 300-370 MPa are possible. For the assessment of these results it should be pointed out, that the shot peening parameters were optimized whereas the laser peening and deep rolling treatments were carried out with non-optimized peening or rolling pressures, respectively. The fatigue strength increase is caused by near-surface compressive residual stresses, work hardening and (for deep rolling) surface smoothening. Microstructural alterations comprise a gradient in the microstructure from the surface to the unaffected core region, i.e. directly under the surface, a partially nanocrystalline region (grain sizes < 100 nm) was detected by ECCI-contrast (Fig. 9), whereas in regions around 5-10 µm distance from the surface ultra-fine grained structures were found. Fig. 8 exhibits EBSD/ECCI pictures of the transition area where a shear elongation of near-surface surface grains as well as increased dislocation densities in rather globular and coarser grains in regions further away from the surface are visible. Highest fatigue strength for CuMn20Ni20 was achieved by a combination of swaging, precipitation hardening and deep rolling (Fig. 10). After this treatment, the fatigue strength could be increased to 600 MPa.

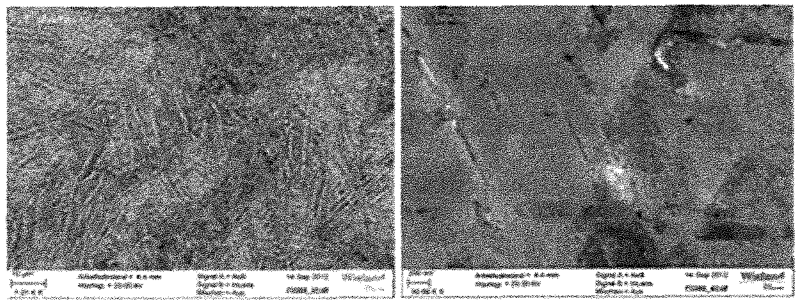

Fig. 3 ECCI overview after swaging plus aging (Left: overview, Right: high resolution)

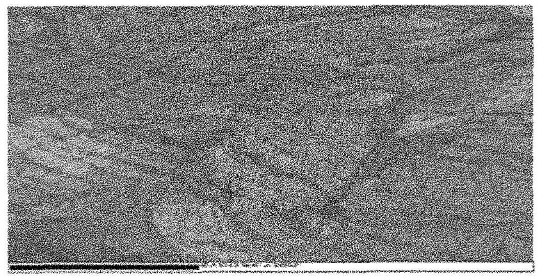

Fig. 4 EBSD orientation map (different colours represent different Euler angles) of theswaged plus aged condition, cross-section

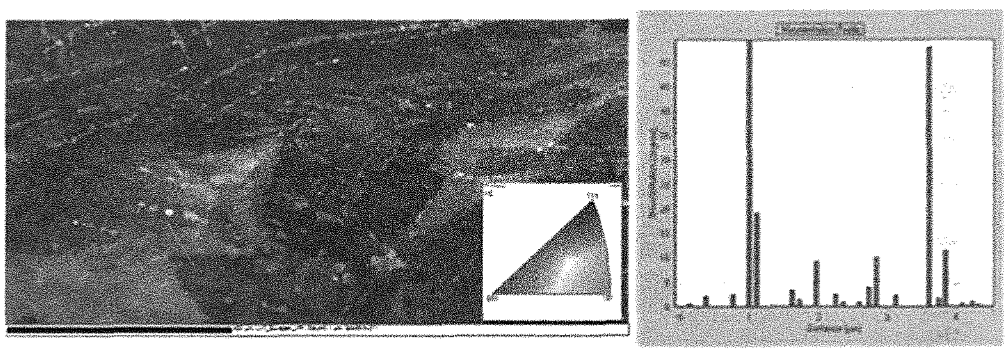

Fig. 5 EBSD orientation map and misorientation profile of the swaged plus aged condition

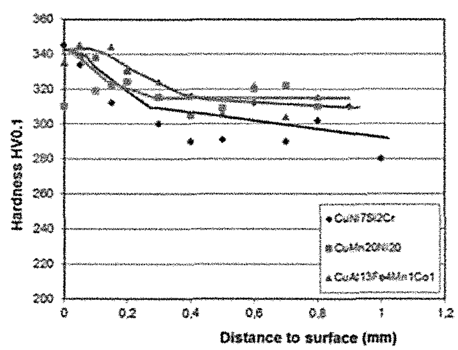

Fig. 6: Hardness increase near the surface by laser peening without coating (three different copper alloys, including aged CuMn20Ni20)

Discussion and Conclusions

Rotary swaging with subsequent artificial aging leads to a complex ultrafine microstructure in spray formed CuMn20Ni20, consisting of 3-deformation twins, nanoscale ordered coherent MnNi-precipitates and high dislocation densities. All of these mechanisms serve to inhibit dislocation movement and limit the mean free path of dislocations. Macroscopically these hardening contributions lead to tensile strengths in excess of 1500 MPa. Rotary swaging is therefore a suitable continuous method of severe plastic deformation (ARB or ECAS [28,29].

Swaging and artificial aging improves the fatigue strength of CuMn20Ni20 only slightly. This can be attributed to the very limited ductility of the peak-aged material and the presence of discontinuous grain boundary precipitates. All investigated treatments such as deep rolling, laser peening without coating or shot peening are able to substantially improve the 10^7-fatigue strength of CuMn20Ni20, especially due to work hardening and near-surface compressive residual stress. If swaging, artificial aging and deep rolling are performed consecutively, fatigue strengths of 600 MPa (under rotary bending) are possible. Explicitly, no separation of strengthening effects by mechanical surface treatment was carried out. However, we assume that for the effect of near-surface compressive residual stress is probably the dominant effect for fatigue strength enhancement, since ultra-hard swaged plus subsequently peak-aged material did not show a strong fatigue strength increase as compared to extruded non-swaged material. Certainly, more work, including residual stress measurements, is needed to delineate exactly the different strengthening contributions.

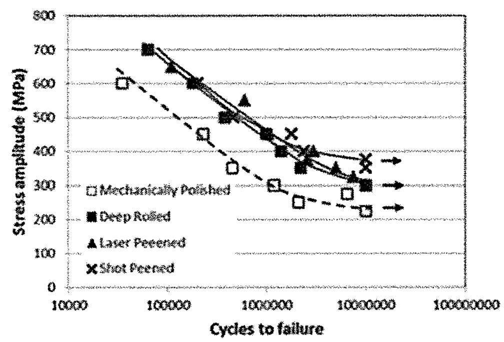

Fig. 7 Effect of surface treatments on fatigue (without swaging)

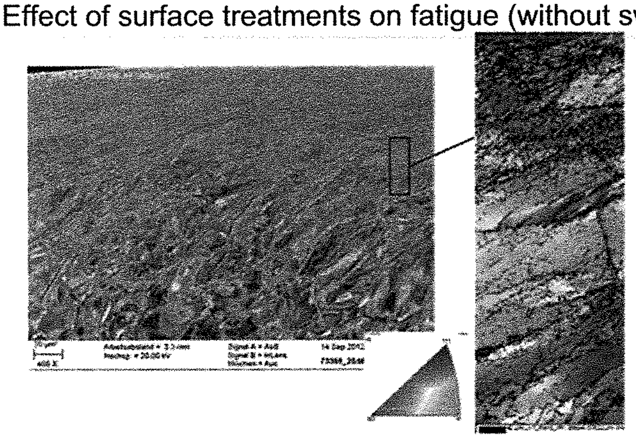

Fig. 8. Orientation mapping of near-surface regions of deep rolled CuMn20Ni20 (distance to surface 60-90 µm). Colours represent orientations from inverse pole figure.

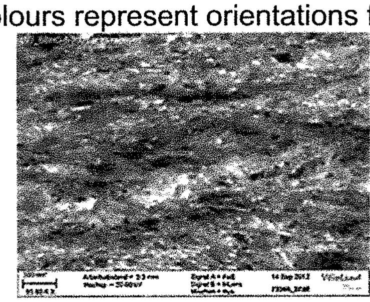

Fig. 9 Nanocrystalline near-surface region of deep rolled CuMn20Ni20 (backscatter contrast, ECCI-micrograph), distance to surface: 1,5 µm

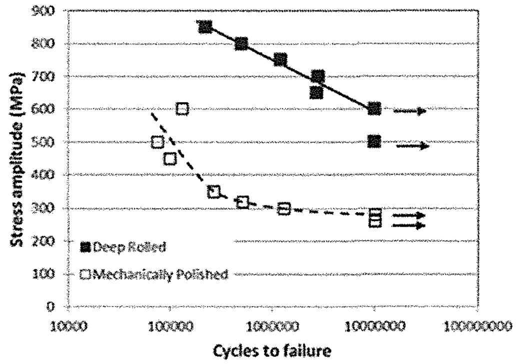

Fig. 10 Effect of deep rolling on fatigue behavior of swaged and aged CuMn20Ni20

References

[1] I. Altenberger, H.R. Müller, R. Zauter, In: Proc. Copper 2010, GDMB, Clausthal-Zellerfeld, 2010, pp 3-12.

[2] S. Shapiro, D.E. Tyler, D. Lanam, In: Proc. CDA-ASM Conf. on Copper, Oct. 16-19, Cleveland, Ohio, 1972.

[3] I. Altenberger, H.-A. Kuhn, H. Hölzl, Prakt. Met. Sonderband, Vol. 44, 2012, p. 52.

[4] I. Altenberger, H.-A. Kuhn, M. Mhaede, M. Gholami, L. Wagner Metall, Vol. 66 (2012), p 500.

[5] Y. Sano, N. Mukai, K. Okazaki, M. Obata, Nuclear Instrum. and Meth. B, Vol. 121 (1997), p. 436.

[6] L. Wagner, M. Mhaede, M. Wollmann, I. Altenberger, Y. Sano, Int. J. Struct. Integrity, Vol. 2 (2011), pp 185-199.

[7] H.-A. Kuhn, I. Altenberger, A. Käufler, H. Hölzl, M. Fünfer, In: Copper alloys – Early applications and current performance – Enhancing processes (Ed. L. Collini), ISBN 978-953-51-0160-4, InTech, 2012, p. 52.

[8] I. Altenberger, H.-A. Kuhn, H. Müller, M. Mhaede, M. Gholami, L. Wagner, Int. J. Mat. Product Tech., 2014, in print.

[9] I. Altenberger, H.-A. Kuhn, M. Gholami, M. Mhaede, L. Wagner, In: Proc. NANO SPD6, Metz, 2014, in print.

[10] V. Schulze, *Modern mechanical surface treatment, Wiley-VCH, Weinheim*, 2006.

[11] L. Wagner, T. Ludian, M. Wollmann, In: Proc. 1st Int. Conf. on Eng. Against Fracture (Eds. S. Pantelakis and C. Rodopoulos), 2009, pp 1-11.

[12] I. Altenberger, I. Nikitin, HTM Härtereitech. Mitt. Vol 59 (2004), pp 269-276.

[13] I. Altenberger, I. Nikitin, *Verfahren zum Verfestigen von Bauteil-Oberflächen durch Festwalzen*, Patent DE 102005041250B4, 29.1.2009.

[14] I. Altenberger, R.K. Nalla, Y. Sano, L. Wagner, R.O. Ritchie, Int. J. Fatigue, Vol. 44 (2012), pp 292-302.

[15] M. Bruder, M.O. Görtan, P. Groche, C. Müller, Mater. Sci. Forum, Vol. 667-669 (2010), pp 103-107.